

# Femtosecond pulse shaping in two dimensions: Towards higher complexity optical waveforms.

V.R. Supradeepa<sup>1</sup>, Chen-Bin Huang<sup>1,2</sup>, Daniel E. Leaird<sup>1</sup> and  
Andrew M. Weiner<sup>1</sup>

<sup>1</sup> School of Electrical and Computer Engineering, Purdue University, West Lafayette, Indiana 47907, USA.

<sup>2</sup> current address: Institute of Photonics Technologies, National Tsing Hua University, Hsinchu, Taiwan.  
[venkatas@purdue.edu](mailto:venkatas@purdue.edu), [robinh@ieee.org](mailto:robinh@ieee.org), [leaird@purdue.edu](mailto:leaird@purdue.edu), [amw@ecn.purdue.edu](mailto:amw@ecn.purdue.edu).

**Abstract:** We demonstrate a new Fourier pulse shaping apparatus capable of achieving simultaneous high resolution and broad bandwidth operation by dispersing frequency components in a two dimensional geometry through simultaneous use of a high resolution and a broad bandwidth spectral disperser. We show experimental results which demonstrate significant improvements in achievable waveform complexity (number of controllable temporal/spectral features). We also demonstrate experiments of line-by-line pulse shaping with optical frequency combs. In this regime our configuration would allow significant enhancement of the number of controllable spectral lines which may further enhance recently demonstrated massively parallel approaches to spectroscopic sensing using frequency combs.

© 2008 Optical Society of America

OCIS codes: (320.0320) Ultrafast optics, (320.5540) Pulse shaping.

---

## References and links

1. M. Weiner, "Femtosecond pulse shaping using spatial light modulators," *Rev. Sci. Instr.* **71**, 1929–1960 (2000).
2. M. Weiner, J. P. Heritage, and E. M. Kirschner, "High-resolution femtosecond pulse shaping," *J. Opt. Soc. Am. B* **5**, 1563-1572 (1988).
3. J. P. Heritage and A. M. Weiner, "Advances in spectral optical code-division multiple-access communications," *IEEE J. Sel. Top. Quantum Electron.* **13**, 1351-1369 (2007).
4. G-H. Lee, S. Xiao, and A. M. Weiner. "Optical Dispersion Compensator with >4000 ps/nm Tuning Range Using a Virtually Imaged Phase Array (VIPA) and Spatial Light Modulator," *IEEE Phot. Tech. Lett.* **18**, 1819-1821 (2006).
5. M. Weiner, D. E. Leaird, G. P. Wiederrecht, and K. A. Nelson. "Femtosecond pulse sequences used for optical manipulation of molecular-motion," *Science* **247**, 1317–1319 (1990).
6. N. Dudovich, D. Oron, and Y. Silberberg, "Single-pulse coherently controlled nonlinear Raman spectroscopy and microscopy," *Nature* **418**, 512–514 (2002).
7. T. Brixner, N. H. Damrauer, P. Niklaus, and G. Gerber, "Photoselective adaptive femtosecond quantum control in the liquid phase," *Nature* **414**, 57–60 (2001).
8. R. J. Levis, G. M. Menkir, and H. Rabitz, "Selective bond dissociation and rearrangement with optimally tailored, strong-field laser pulses," *Science* **292**, 709–713 (2001).
9. R. Bartels, S. Backus, E. Zeek, L. Misoguti, G. Vdovin, I. P. Christov, M. M. Murnane, and H. C. Kapteyn, "Shaped-pulse optimization of coherent emission of high-harmonic soft X-rays," *Nature* **406**, 164–166 (2000).
10. M. Shirasaki, "Large angular dispersion by a virtually imaged phased array and its application to a wavelength division multiplexer," *Opt. Letters.* **21**, 366–368 (1996).
11. S. Xiao and A. M. Weiner, "2-D wavelength demultiplexer with potential for >= 1000 channels in the C-band," *Opt. Express* **12**, 2895-2902 (2004).
12. S. X. Wang, S. Xiao, and A. M. Weiner. "Broadband, High Spectral Resolution 2-D Wavelength-Parallel Polarimeter for Dense WDM Systems," *Opt. Express* **13**, 9374-9380 (2005).
13. S. A. Diddams, L. Hollberg, and V. Mbele, "Molecular fingerprinting with the resolved modes of a femtosecond laser frequency comb," *Nature* **445**, 627-630 (2007).
14. [http://www.holoeye.com/phase\\_only\\_modulator\\_heo1080p.html](http://www.holoeye.com/phase_only_modulator_heo1080p.html)

15. T. Hornung, J. C. Vaughan, T. Feurer, and K. A. Nelson. "Degenerate four-wave mixing spectroscopy based on two-dimensional femtosecond pulse shaping," *Opt. Letters*. **29**, 2052-2054 (2004).
16. R. P. Scott, W. Cong, V. J. Hernandez, K. Li, B. H. Kolner, J. P. Heritage, and S. J. B. Yoo, "An Eight-User Time-Slotted SPECTS O-CDMA Testbed: Demonstration and Simulations," *J. Lightwave Technol.* **23**, 3232- (2005).
17. E. Frumker and Y. Silberberg, "Femtosecond pulse shaping using a two-dimensional liquid-crystal spatial light modulator," *Opt. Lett.* **32**, 1384 (2007).
18. C.-B. Huang, Z. Jiang, D. E. Leaird, and A. M. Weiner, "High-Rate Femtosecond Pulse Generation via Line-by-Line Processing of a Phase-Modulated CW Laser Frequency Comb," *Electron. Lett.* **42**, 1114-1115 (2006).
19. V. R. Supradeepa, E. Hamidi, D. E. Leaird, and A. M. Weiner, "New aspects of temporal dispersion in virtually imaged phased array (VIPA) based Fourier pulse shapers," CThDD3, CLEO 2008.
20. Z. Jiang, D. S. Seo, D. E. Leaird, and A. M. Weiner, "Spectral line by line pulse shaping," *Opt. Letters*. **30**, 1557-1559 (2005).
21. D. J. Jones, S. A. Diddams, J. K. Ranka, A. Stentz, R. S. Windeler, J. L. Hall, and S. T. Cundiff, "Carrier-envelope phase control of femtosecond mode-locked lasers and direct optical frequency synthesis," *Science* **288**, 635-639 (2000).
22. T. Udem, R. Holzwarth, and T. W. Hansch, "Optical frequency metrology," *Nature* **416**, 233-237 (2002).
23. M. C. Stowe, F. Cruz, A. Marian, and J. Ye. "High Resolution Atomic Coherent Control via Spectral Phase Manipulation of an Optical Frequency Comb," *Phys. Rev. Lett.* **96**, 153001 (2006).
24. Marian, M. C. Stowe, J. Lawall, D. Felinto, and J. Ye. "United Time-Frequency Spectroscopy for Dynamics and Global Structure," *Science* **306**, 2063-2068 (2004).
25. Z. Jiang, C.-B. Huang, D. E. Leaird, and A. M. Weiner, "Optical Arbitrary Waveform Processing of More than 100 Spectral Comb Lines," *Nature Photon.* **1**, 463-467 (2007).
26. R. P. Scott, N. K. Fontaine, J. Cao, K. Okamoto, B. H. Kolner, J. P. Heritage, and S. J. B. Yoo, "High-fidelity line-by-line optical waveform generation and complete characterization using FROG," *Opt. Express* **15**, 9977-9988 (2007).
27. D. Miyamoto, K. Mandai, T. Kurokawa, S. Takeda, T. Shioda, and H. Tsuda, "Waveform-Controllable Optical Pulse Generation Using an Optical Pulse Synthesizer," *IEEE Photon. Technol. Letters*. **18**, 721-723 (2006).
28. Lohmann and D. P. Paris, "Binary Fraunhofer holograms, generated by computer," *Appl. Opt.* **6**, 1739 (1967).
29. M. Weiner, D. E. Leaird, D. H. Reitze, and E. G. Paek, "Femtosecond spectral holography," *IEEE JQE* **28**, 2251 (1992).
30. J. W. Wilson, P. Schlup, and R. A. Bartels. "Ultrafast phase and amplitude pulse shaping with a single, one-dimensional, high-resolution phase mask," *Opt. Express* **15**, 8979 - 8988 (2007).

## 1. Introduction

Femtosecond pulse shaping is a technique which allows generation of user-specified optical waveforms by parallel manipulation of the complex optical spectrum[1,2] and has been widely adopted in applications ranging from optical communications to coherent control of quantum processes[3-9]. In a conventional Fourier pulse shaping apparatus, the spectrum of an incident pulse is spread along one spatial dimension and focused onto a spatial light modulator (SLM), which transfers spatial phase and amplitude information onto the complex optical spectrum. This Fourier synthesis procedure results, after the optical frequencies are recombined, in programmable user-defined ultrashort pulse waveforms. In order to generate higher complexity optical waveforms, two qualities are desired: a) enhanced spectral resolution, which corresponds to an increased temporal aperture for waveform control, and b) broad operational bandwidth, which translates into fine temporal features. Currently employed spectral dispersers require a compromise between achievable resolution and available bandwidth. This is a fundamental limitation in optical arbitrary waveform generation which requires simultaneously both a broad operational bandwidth and high spectral resolution.

To circumvent this problem, we introduce a new pulse shaping configuration that takes advantage of both a broadband spectral disperser and a high resolution disperser. As the broadband disperser we use a diffraction grating, which is the most common choice for 1D pulse shapers. As the high resolution disperser, we choose a virtually-imaged phased array (VIPA)[10] - a side entrance Fabry-Perot device that achieves spectral dispersion through

multiple beam interference. We have recently reported a programmable 1D pulse shaper based on a VIPA spectral disperser that achieves ~700 MHz spectral resolution – a significant enhancement compared to grating based shapers[4]. However, similar to a Fabry-Perot cavity, the VIPA is characterized by a free spectral range (FSR), at most a few hundred GHz for available VIPAs, which limits the bandwidth over which spectra may be independently manipulated. Here, by using a VIPA and a grating together in a cross-dispersion configuration which spreads light in 2D, we simultaneously achieve both high resolution and broadband operation. This 2D spectral dispersion arrangement has been reported for experiments in optical communications wavelength demultiplexing[11], wavelength-parallel polarization sensing[12], and frequency-comb spectroscopy[13], but prior to now has not been demonstrated for optical pulse shaping. An additional benefit of pulse shaping in a 2D geometry is the potential to exploit modern SLM technologies, which already can provide more than two million control pixels in a 2D format[14], compared to 1D SLMs with hundreds of pixels typically and at most a few thousand.

Although previous demonstrations of pulse shaping in a 2D geometry have been reported[15-17] these have been performed with a single spectral disperser (a grating) and have not been directed towards enhancing time-frequency complexity. For example, single disperser 2D pulse shapers have been used for simultaneous generation of multiple spatially separated waveforms for applications such as four-wave mixing spectroscopy[15] and multiple-access ultrashort pulse communications[16]. In another example, galvanometric scanning between different rows of a 2D SLM has been used to achieve faster waveform switching in pulse shaping[17]. In the current approach the entire two dimensional space is used to disperse and control the frequency components corresponding to a single target waveform, which translates into potential for very high waveform complexity.

## 2. Experimental setup

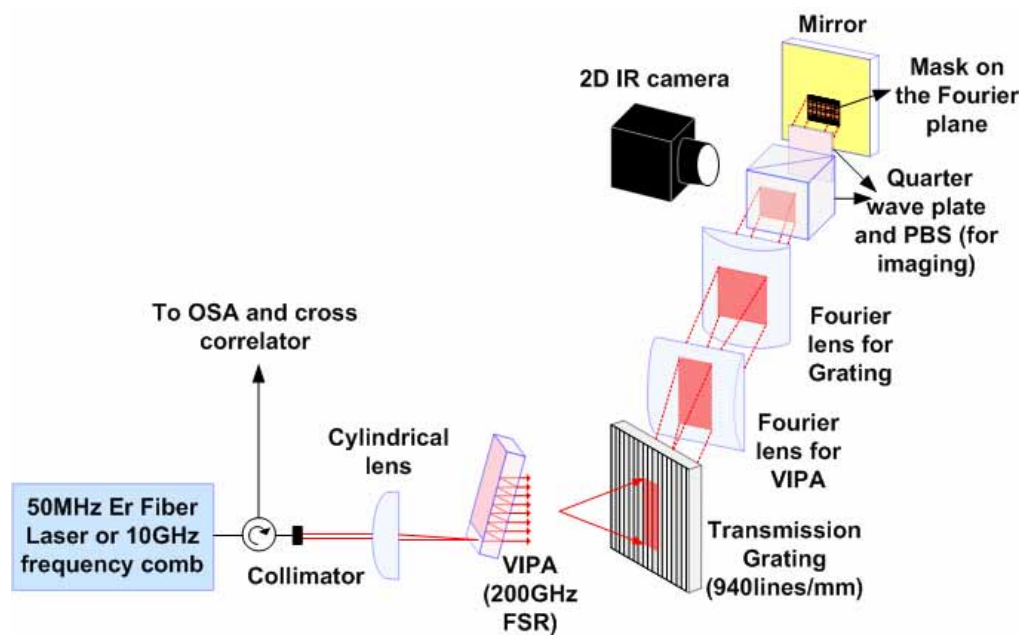


Fig. 1. The experimental setup - after undergoing dispersion by the VIPA (free spectral range (FSR) of 200GHz) and the grating (940lines/mm) in perpendicular directions, and spatial Fourier transforms by the respective lenses, the light forms a 2D pattern on the Fourier plane

where a patterned mask shapes the input spectrum. An adjustable fraction of the light is diverted to an imaging camera for aligning and monitoring the mask.

Figure 1 shows the experimental setup. Our experiments utilize either a 50MHz repetition rate mode-locked erbium fiber laser generating 150 fs bandwidth-limited pulses or a 10 GHz repetition rate optical frequency comb consisting of more than 500 comb lines (within 30dB) corresponding to bandwidth-limited 300 fs pulses[18]. The pulse shaper consists of a VIPA-grating spectral disperser, cylindrical lens focusing elements, and a retroreflecting mirror, with the output extracted through an optical circulator. In the absence of masking at the Fourier plane, the setup has been aligned so that the output spectrum and temporal intensity cross-correlation are identical to those measured at the input. The VIPA used is air spaced and has a FSR of 200GHz. The transmission grating has a pitch of 940 lines/mm. After the VIPA and the grating, two cylindrical lenses are used, one for each of the dispersers. This step is necessary because of the need to obtain a zero net temporal dispersion configuration for either spectral disperser independently. Reflective grating based pulse shapers employ a single lens in a 4-f configuration, where the grating-lens and lens-mirror distances are each set equal to the focal length for zero net temporal dispersion. However, VIPA based pulse shapers require a different distance to have zero temporal dispersion[19]. Hence, to achieve net zero dispersion for both dispersers together, the degree of freedom offered by using two lenses is necessary. The total loss of the pulse shaper including the circulator was ~15dB. To better represent this number, VIPA only pulse shapers have a loss of ~12dB; the increase in loss moving to a 2D setup is approximately 3dB.

For this current set of experiments, we implement pulse shaping using an amplitude mask that is patterned in 2D using standard photolithographic techniques. In a two dimensional configuration, there is an additional alignment degree of freedom necessary to put the mask in correct orientation. Therefore, a continuous real-time monitoring tool is essential to properly orient the mask. This monitoring was provided by the IR camera which imaged the Fourier plane of the pulse shaper. A polarizing beam splitter followed by a quarter wave plate makes it possible to control the amount of power going to the camera and minimizes losses for the shaper. The 2D IR camera used in these experiments to obtain the images of the Fourier plane acquires images in a grey scale format. Minor processing has been performed on the images to be shown in the following figures which include reducing the ambient noise, increasing the contrast, and changing the color scheme to improve readability of the images. Otherwise, the images are exact representations of the Fourier plane in the experiment.

Figure 2(a) shows the Fourier plane image for the 50MHz repetition rate Erbium fiber laser source without masking. In the figure, all the frequency components of the input source are present and the image appears to be continuous streaks which are different VIPA FSRs spatially separated by the grating. The laser repetition rate of 50MHz is significantly smaller than the spectral resolution in our setup which is ~3GHz ;hence, though the spectrum consists of discrete frequency components, the Fourier plane image appears as continuous streaks. Fig. 2(b) shows the Fourier plane image with an amplitude mask designed to introduce both coarse and fine features into the optical spectrum, while also suppressing all but the main diffraction order of the VIPA. Ideally the mask can be made to simultaneously shape identical frequency components from different orders, however this is difficult to achieve in a fixed mask configuration (without programmable control) and so in our current set of experiments we block all the VIPA orders except the dominant order.

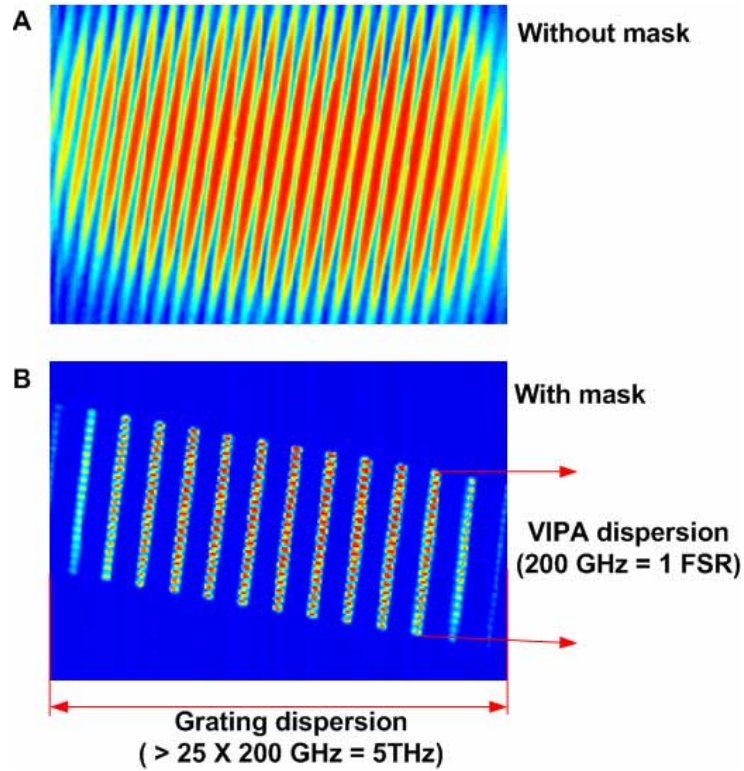


Fig. 2. (a) Image of the Fourier plane without a mask, (b), with a mask.

### 3. Experimental results

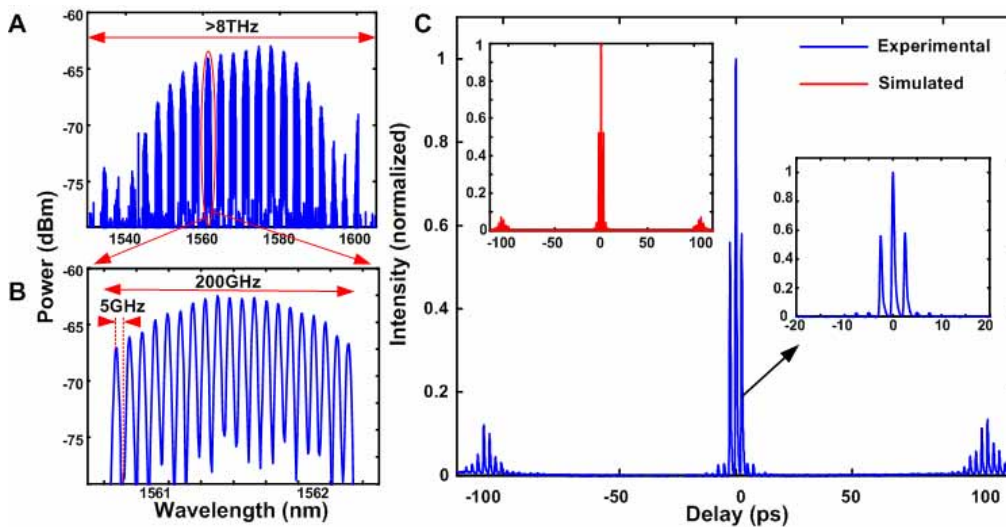


Fig. 3. (a), the full spectrum of the shaped pulse. (b), magnified portion of the spectrum circled in red in Fig. 3(a). The smallest features are 5GHz, and over a bandwidth of 8THz ( $> 64\text{nm}$ ), there are more than 1600 controllable spectral features. (c), time domain cross correlation trace. An initially bandwidth limited pulse of 150fs is shaped over a time window exceeding 200ps.

Figure 3(a) shows an OSA measurement of the shaped spectrum, and Fig. 3(a) shows a magnified view of one FSR (circled in red in Fig. 3(a)) corresponding to the mask shown in Fig. 2(a). The mask blocks out every alternate FSR of the VIPA (indicated in the image by a doubling of the FSR-to-FSR spacing), introducing a coarse periodicity of 400 GHz. Within each transmitted FSR the mask creates on-off sections with a width of 5 GHz each (hence a 10 GHz fine periodicity). The magnified portion of the spectrum in Fig. 3(b) shows this on-off operation within a single FSR. The initial 10dB bandwidth covers more than 8 THz (>64nm). With the 5 GHz minimum feature size, the spectrum contains more than 1600 potentially controllable features, corresponding to substantially higher complexity than any previous pulse shaping demonstration to the best of our knowledge. The intensity cross-correlation trace shown in Fig. 3(c) demonstrates that the initial 150 fs pulse is now redistributed over a total time aperture of more than 200ps. The inset in red shows the simulated output which is in excellent agreement with the measurement. A small amount of 2<sup>nd</sup> and 3<sup>rd</sup> order spectral phase was added to the simulations of shaped waveforms to take into account the small residual dispersion of the dispersion compensated fiber links. The same residual phase value was maintained for all simulations and was initially obtained by comparing the calculated cross-correlation assuming flat spectral phase with the cross-correlation of the pulse shaper output without any applied mask. The second inset shows the fine temporal features near the main pulse which arise due to the coarse periodicity in the mask. Even greater pulse shaping complexity is possible using this apparatus, limited in the present experiments by the input optical bandwidth.

Figure 4 shows an example of a pure spectral shaping experiment. Figure 4(b) shows OSA spectra obtained with the two masks whose images are shown in Fig. 4(a). Complicated structure is observed, with features as fine as 10 GHz spread over 4.5THz of bandwidth. Figure 4(c) shows the same spectra, replotted in a row-column format, with one FSR (200GHz) per row and three columns per spectrum. Now an image emerges from the OSA spectra, spelling out the word 'PURDUE.' This example illustrates the direct correspondence between the applied spatial mask and the spectral transfer function and demonstrates the ability to achieve nearly arbitrary intensity control of the optical spectrum.

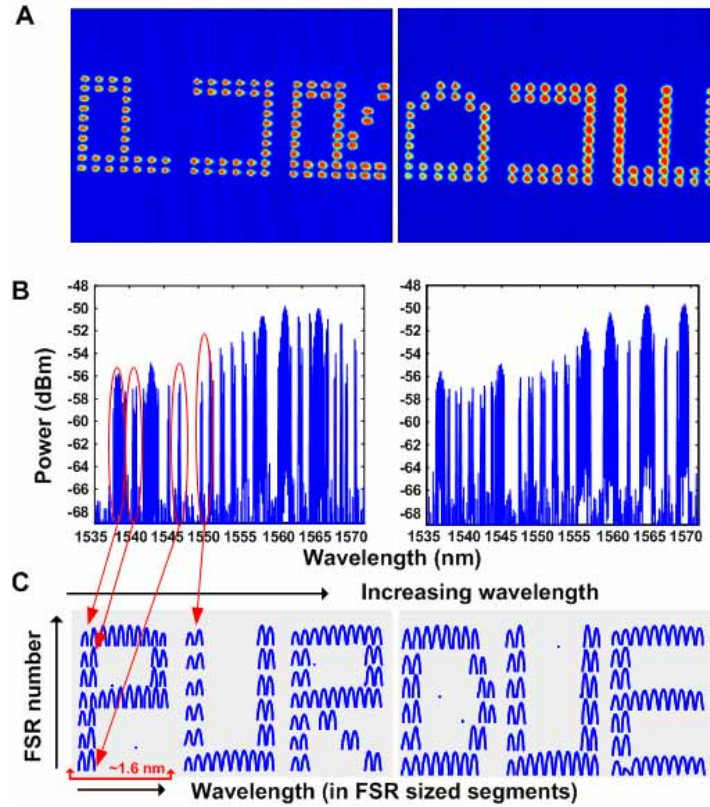


Fig . 4. (a), images of the Fourier plane for the two halves of the mask; the corresponding spectra are shown in (b). The smallest spectral feature is 10GHz and the total number of features in either spectra is around 450. To better represent the features determined by the mask, both spectra are split into three sections, each consisting a few FSRs of the VIPA. Each section is then plotted in segments of one FSR (200 GHz) lined vertically as shown in (c). The clear correspondence between the applied mask and the spectrum demonstrates enhanced spectral control made possible by the ability to control fine spectral features over a large bandwidth.



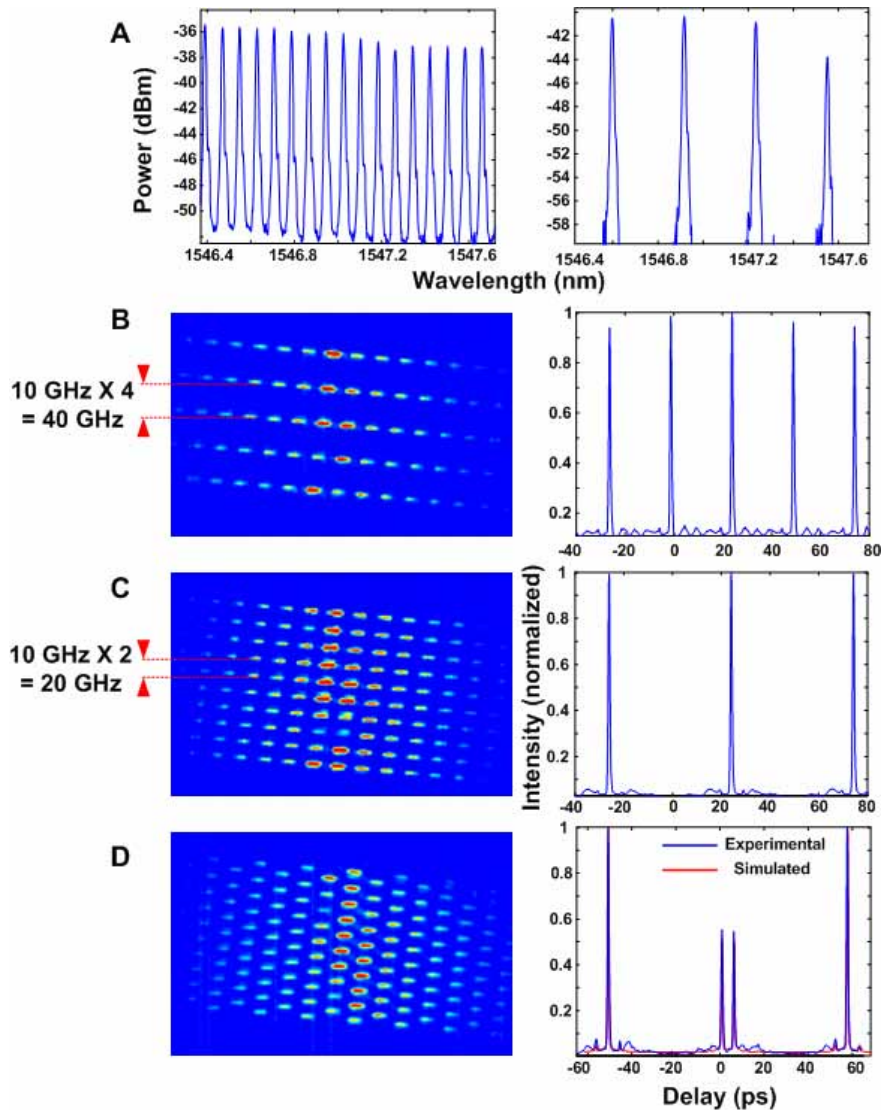


Fig. 5. (a) a portion of the input frequency comb and the same section after application of a pulse rate quadrupling mask. The line-to-line spectral spacing of the input is 10GHz, which is the temporal repetition rate of the source. After application of the mask, the line-to-line spacing is manipulated to be 40GHz. (b), the image of the Fourier plane with the quadrupling mask and the corresponding time domain cross correlation trace. The pulse-to-pulse separation is 25ps corresponding to the 40GHz repetition rate. (c), a pulse rate doubling experiment. The image of the Fourier plane shows spot-to-spot separation equal to half of that shown in (b), corresponding to a frequency comb of 20GHz separation. In the time domain the pulse-to-pulse separation is 50ps as expected. In D, a mask is utilized which is a slight modification of the pulse rate doubling mask. This is indicated by the spot-to-spot separation being similar to C, but the pattern is staggered by inserted irregularities every 20 spectral lines. In the time domain this results in a significant change, where a double pulse structure is observed near zero delay instead of a single pulse as in the pulse rate doubling case (c). Excellent agreement between the simulated (red) and the experimental (blue) cross correlation traces is observed.

An important application for the 2D shaper is in the regime of line-by-line pulse shaping[20], in which discrete spectral lines from an optical frequency comb[21,22] are individually manipulated. Our pulse shaping configuration allows for significant enhancement of the number of controllable frequency lines. This regime is particularly



interesting because optical frequency combs, consisting of a large number of discrete spectral lines, are already enabling massively parallel novel approaches to spectroscopic sensing[23,24], approaches which potentially may be further enhanced by amplitude and phase control of the individual comb lines.

To generate a frequency comb for these experiments, a single-frequency continuous-wave (CW) laser is converted to a 40 line frequency comb by an integrated optic phase modulator strongly driven by a 10GHz sinusoid[20,25-27]. However, the phases of the frequency components are not the same, and the intensity remains constant in time. A bandwidth-limited pulse is obtained by phase correcting individual frequency components in a high resolution line-by-line pulse shaper by maximizing the second harmonic generation signal from an autocorrelator set at zero delay as the phase of individual frequency components is adjusted. After phase correction, the output pulse is found to be in excellent agreement with the pulse simulated assuming flat spectral phase. The bandwidth-limited pulses are passed through a dispersion decreasing fiber (DDF) adiabatic soliton compressor, which broadens the 30dB bandwidth to 40 nm and increases the number of lines in the comb to 500. The autocorrelation of the spectrally broadened pulses was again found to be in good agreement with the autocorrelation simulated on the basis of a flat spectral phase assumption.

Figure 5(a) presents a small section of the spectrum both before and after applying a pulse rate quadrupling mask. After applying the mask, the initial 10 GHz comb spacing is increased to 40GHz. Figure 5(b) shows the image of the masked Fourier plane and the corresponding time domain cross correlation trace. The discrete or comb-like nature of the optical spectrum is evident as discrete spots at the Fourier plane. The central spots are brighter due the shape of the source spectrum. In the time domain, the pulse-to-pulse separation is 25ps corresponding to the 40GHz line spacing determined by the mask. Fig. 5(c) shows the image of the Fourier plane with a pulse rate doubling mask and the corresponding time domain trace. In the time domain, pulses repeating every 50ps are observed as expected. In Fig. 5(d), a slight modification of the pulse rate doubling mask is implemented: at the edge of every FSR, two successive lines are either selected or skipped. This modification significantly reshapes the time domain output: instead of a single pulse at the midpoint of the cross-correlation, a pulse doublet is now observed. The trace shown in red is the simulated output, which is in excellent agreement with the experimental cross-correlation.

Figure 6 demonstrates a final interesting example which begins to exploit spectral phase. Because the masking operation implemented currently is strictly amplitude-only, we follow a design approach based on computer generated holography[28], where phase information is encoded as a slow modulation in the periodicity of a nearly periodic amplitude pattern. In our experiment the mask modulates the initial spectrum in an on-off fashion, with a period that varies slowly over the optical bandwidth. This results in a mixture of quadratic and cubic spectral phase, which may be discerned qualitatively from the curvature evident in the Fourier plane image (inset). Readout of this spectral hologram[29] results in a time domain trace consisting of an unshaped peak at  $t=0$  with equal but time-reversed shaped signals at positive and negative time offsets, respectively. These features correspond to the undiffracted zero-order beam and to the real and conjugate images generated from 1<sup>st</sup>- and -1<sup>st</sup>-order diffraction in the spatial holography analog. Here in our time domain experiment, the satellite pulses exhibit a clear asymmetric tail as expected from the designed cubic spectral phase as well as a small broadening associated with quadratic phase.

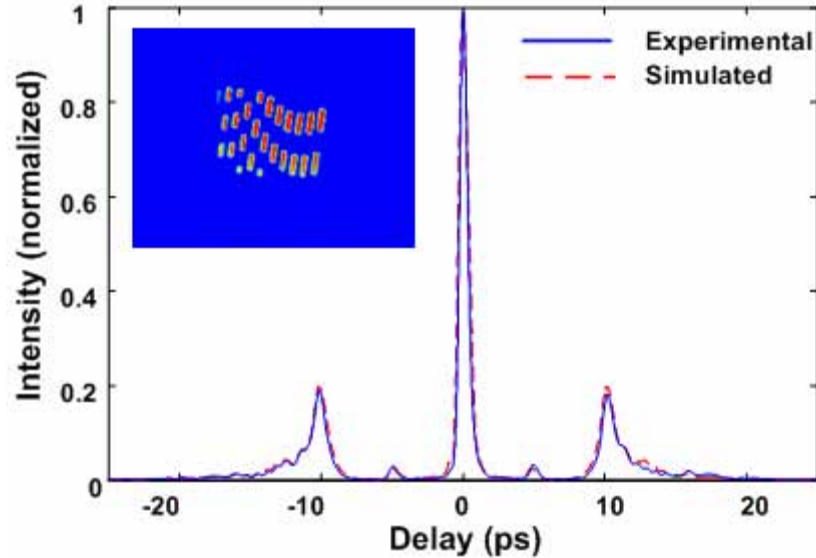


Fig. 6. An experimental cross correlation trace (solid blue) and the simulated (dashed red) trace are superimposed; excellent agreement between the two traces is observed. Both satellite pulses have been broadened, indicating a quadratic spectral phase with the acquired tail indicating a cubic spectral phase. The image on the inset shows the Fourier plane with the mask in place.

#### 4. Summary and future work

In closing, we have demonstrated a fundamentally new pulse shaping geometry which disperses optical frequencies along a two-dimensional grid, resulting in a substantial increase in achievable pulse shaping complexity. It should be possible to scale this scheme for high spectral resolution shaping of octave spanning optical sources. For example, for a 10 GHz repetition rate, octave spanning laser frequency comb centered at  $1.55 \mu\text{m}$  wavelength, independent control of the approximately twenty thousand spectral lines comprising the comb should be possible. Our 2D pulse shaping geometry offers compatibility with 2D spatial light modulators developed for display applications, which currently offer in excess of two million control pixels. Although such SLMs typically offer direct access only to optical phase (for example), the large surplus of available control pixels may be harnessed for diffractive schemes allowing independent gray-level amplitude and phase control, as demonstrated recently in a 1D pulse shaping experiment[30]. In future work we plan to integrate such 2D SLMs into our apparatus, which should yield arbitrary and fully programmable manipulation of complex optical spectra for generation of precisely tailored but enormously complex ultrafast optical waveforms.

#### Acknowledgments

We would like to thank Avanex corporation for the VIPAs devices and acknowledge support from the National Science Foundation under grant ECCS-0601692, and DARPA/ARO under grant FA9550-06-1-0189.